

High resolution Spectra of Earth-Like Planets Orbiting Red Giant Host Stars

Thea Kozakis, Lisa Kaltenegger

Carl Sagan Institute, Cornell University, Ithaca, NY 14853

ABSTRACT

In the near future we will have ground- and space-based telescopes that are designed to observe and characterize Earth-like planets. While attention is focused on exoplanets orbiting main sequence stars, more than 150 exoplanets have already been detected orbiting red giants, opening the intriguing question of what rocky worlds orbiting in the habitable zone of red giants would be like and how to characterize them. We model reflection and emission spectra of Earth-like planets orbiting in the habitable zone of red giant hosts with surface temperatures between 5200 and 3900 K at the Earth-equivalent distance, as well as model planet spectra throughout the evolution of their hosts. We present a high-resolution spectral database of Earth-like planets orbiting in the red giant habitable zone from the visible to infrared, to assess the feasibility of characterizing atmospheric features including biosignatures for such planets with upcoming ground- and space-based telescopes such as the Extremely Large Telescopes and the James Webb Space Telescope.

Subject headings: Astrobiology, Exoplanet atmospheres, Exoplanet evolution, Habitable zone, Habitable planets, Stellar evolution, Evolved stars, Red giant stars, Horizontal branch, Biomarkers

1. Introduction

Although the majority of detected exoplanets orbit main sequence (MS) stars, over 150 exoplanets have already been found around red giant (RG) stars (i.e. Jones et al. 2014; Lopez, & Fortney 2016; Grunblatt et al. 2017; Jiang, & Zhu 2018). The characteristics of rocky planets and moons in the post-MS habitable zone (HZ) around RGs are unknown and such places could be interesting to search for life (see e.g. Lorenz et al. 1997; Stern 2003; Ramirez, & Kaltenegger 2016; Kozakis & Kaltenegger 2019). Un-

til now there have been no spectral models of such planets or moons to explore how to characterize them remotely as well as assess detectability of biosignature for such worlds.

When a star exhausts their core hydrogen and leaves the MS, its surface cools and expands, increasing overall luminosity and engulfing their inner planetary systems. However, during this time period the orbital distance of their HZ increases past the system's original frost line, where 99.99% of the solar system's water resides (e.g. Stern 2003), suggesting that initially frozen rocky worlds could thaw and become partially to fully

ocean-covered worlds during the RG phase of their host star (e.g. Lorenz et al. 1997; Stern 2003; Ramirez, & Kaltenegger 2016; Kozakis & Kaltenegger 2019).

The post-MS HZ orbital distance changes significantly during the hydrogen shell fusion on the RG branch (RGB), becomes stable during helium core fusion on the horizontal branch (HB), and returns to rapidly changing on the asymptotic giant branch (AGB) where both hydrogen and helium shell fusion occur. During this period of stability on the HB planets can remain continuously in the post-MS RG HZ for up to 257 Myr (Kozakis & Kaltenegger 2019). Although life might need longer than that time span to originate, with estimates ranging from 0.5 to 1 Gyr (e.g. Furnes et al. 2004; Lopez et al. 2005), subsurface life could evolve under an ice shell during the MS. Such an ice layer could melt during its host star’s RG evolution and could reveal such biota through remote observations (Ramirez, & Kaltenegger 2016). In our own solar system, both Jupiter and Saturn will remain in the post-MS HZ for the majority of the HB, making moons such as Europa, Enceladus, and Titan interesting bodies for future temperate surface conditions in the solar system (see e.g. Lorenz et al. 1997; Stern 2003; Ramirez, & Kaltenegger 2016; Kozakis & Kaltenegger 2019).

Several studies explored the nature of the post-MS HZ (e.g. Stern 2003; Lopez et al. 2005; Barnes, & Heller 2013; Danchi, & Lopez 2013; Ramirez, & Kaltenegger 2016; Yang et al. 2017) and the resulting planetary atmospheres (Kozakis et al. 2018; Kozakis & Kaltenegger 2019), but no work had been done to quantify the spectra as well as detectability of biosignatures for Earth-like planets orbiting RG stars. Due to the wide orbital separation of the RG HZ, the spectra of such planets could be directly assessed in reflection and emission. Assessing biosig-

nature detectability around a wide range of host stars (for MS stars see e.g. reviews by Des Marais et al. (2002); Kaltenegger et al. (2007); Schwieterman et al. (2018)) is particularly relevant with missions on the horizon that are designed to characterize rocky planet atmospheres, namely JWST (Gardner et al. 2006), ELT (Gilmozzi, & Spyromilio 2007), and future mission concepts like ARIEL (Tinetti et al. 2016), Origins (Battersby et al. 2018), HabEx (Mennesson et al. 2016), and LUVOIR (Bolcar et al. 2016).

While the orbital distance of the RG HZ increases significantly due to the higher luminosity of the host RG, increasing the apparent angular separation of such planets compared to MS HZ planets, the contrast ratio between such planets and their RG hosts are also smaller than for similar planets orbiting in the HZ of MS stars. However ground-based high resolution spectroscopy has already characterized atmospheric species for unresolved planets like HD 179949 b using the planet’s known motion during the observations (e.g. Snellen et al. 2013; Brogi et al. 2014; Birkby 2018). A similar approach could be used to counter the increased luminosity of RG hosts to observe their HZ planets, making such planets interesting targets for observations with Extremely large Telescopes.

In this study we present spectra for Earth-like planets in the RG HZ both i) at the Earth-equivalent distance and ii) for several points throughout the RG’s evolution for stellar mass tracks of 1.3, 2.3 and 3.0 M_{\odot} . For a detailed model description see Kozakis & Kaltenegger (2019), which discusses the planetary atmospheric models and their corresponding UV surface environments. These models include planetary atmospheric erosion as well as semimajor axis evolution resulting from its host’s mass loss during the RG phase (Kozakis & Kaltenegger 2019).

Table 1: Properties of the red giant hosts

Spectral Type	Star Name	Star T_{eff} (K)	Dist. (pc)	Radius (R_{\odot})	Planet T_{surf} (K)	1 AU equiv. dist (AU)	Mass track (M_{\odot})	a for max HZ (AU)*
G5 III	HD 74772	5118	70.18	12.90	289.3	10.12	3.0	18.2
G8 III	HD 148374	4948	155.28	14.52	294.5	10.65	3.0	18.2
K0 III	β Gem	4865	10.36	8.8	295.0	6.24	2.3	12.0
K0 III	β Ceti	4797	29.5	16.78	295.5	11.57	3.0	18.2
K2 III	ι Draconis	4445	31.03	11.99	298.6	7.10	1.3	12.5
K2 III	θ Doradus	4320	151	16	299.1	8.94	1.3	12.5
K3 III	α Boo	4286	11.26	25.4	303.6	13.98	2.0	12.2
K5 III	γ Draconis	3989	47.3	53.4	304.7	25.45	2.3	12.0

*Semimajor axis values correspond to a planet’s initial orbital position resulting in the maximum amount of time in the HZ of its RG host, taking stellar mass loss and planetary orbit changes into account.

Due to the wide orbital separation of the HZ around luminous RGs, planetary atmospheric mass loss via erosion is limited to less than 10% for planets with a 1 bar surface pressure (ibid). A summary of RG hosts and their HZ model data from Kozakis & Kaltenegger (2019) is shown in Table 1.

Section 2 describes our methods, Section 3 discusses the spectra of planets in the post-MS HZ at Earth-equivalent distance as well as throughout their host’s RG evolution, and Section 4 discusses and concludes our paper.

2. Methods

2.1. Stellar hosts and planet atmospheric spectra models

We model Earth-like planet reflection and emission spectra orbiting 8 different RG stars. Their incident stellar spectra consist of combined IUE¹ UV and Pickles Atlas (Pickles 1998) luminosity class III spectra (see Table 1 and Figure 1). Evolutionary phase and mass track were estimated using results from Stock et al. (2018) and H-R diagram fitting. For a full description of these stellar spectra see Kozakis & Kaltenegger (2019).

We created the planetary atmosphere models and high resolution spectra using *Exo-Prime* (e.g. Kaltenegger et al. 2010), a 1D coupled climate-photochemistry-radiative transfer code developed for terrestrial planets.

For each planetary atmospheric model, described in Kozakis & Kaltenegger (2019), *Exo-Prime* generates a high resolution reflection and emission spectra in wavenumber steps of 0.01 cm^{-1} from 0.4 to $20 \text{ }\mu\text{m}$, using a line-by-line radiative transfer model originally developed to retrieve trace gases in Earth’s atmosphere (Traub & Stier 1976) and later adapted to simulate emergent and transmission exoplanet spectra (e.g. Kaltenegger et al. 2007, 2013). For each atmospheric layer line shapes and widths are calculated individually with Doppler- and pressure-broadening with several points per line width. We include the most spectroscopically relevant molecules in our calculations: H_2O , CO_2 , N_2O , NO_2 , HNO_3 , O_3 , CH_4 , O_2 , CO , OH , H_2CO , CH_3Cl , and O , as well as Rayleigh scattering. We use a Lambert sphere approximation for a disk-integrated planet and model Earth-like surfaces for clear sky and 60% coverage of Earth-like clouds (following Kaltenegger et al. 2007). Our Earth surface consists of 70% ocean, 2% coast, and 28% land, with the land comprised of 30%

¹<http://archive.stsci.edu/iue/>

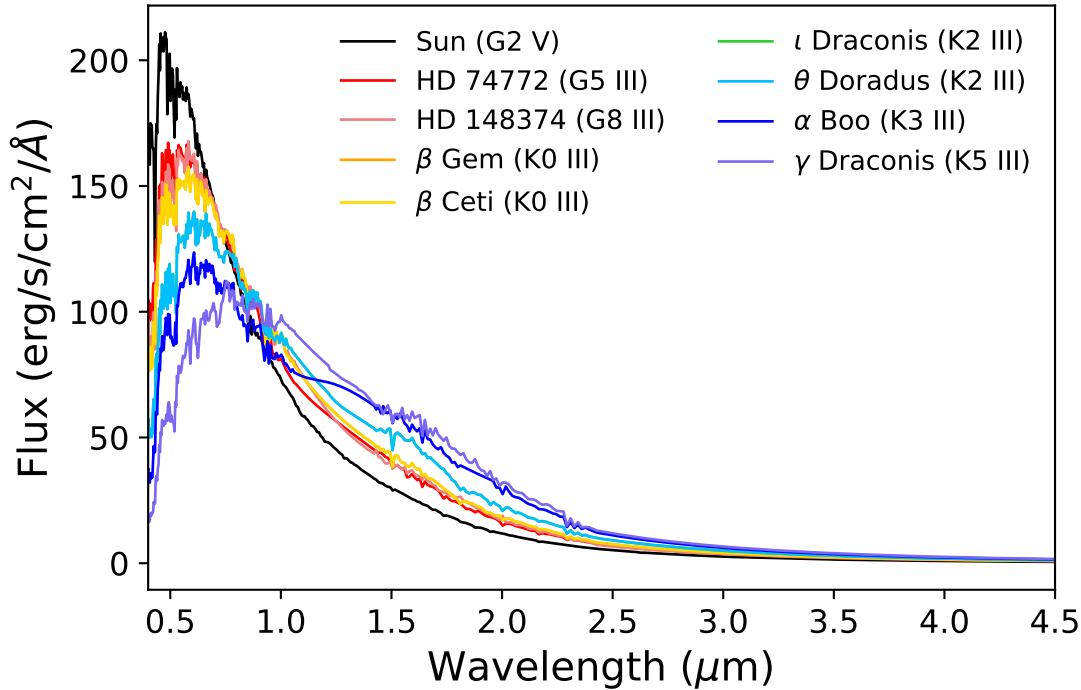


Fig. 1.— Incident stellar spectra of the red giant hosts scaled to the 1 AU-equivalent distance, shown at a resolution of $R = 140$. Red giants with cooler surface temperatures show longer peak wavelengths as well as additional spectral lines due to molecular formation in their atmospheres. See Table 1 for information on individual targets.

grass, 30% trees, 9% granite, 9% basalt, 15% snow, and 7% sand. The 60% coverage by Earth-like clouds assumes a distribution of clouds with 40% at 1 km, 40% at 6 km, and 20% at 12 km. All albedo data are from the USGS Digital Spectral Library² and the ASTER Spectral Library³.

All spectra can be downloaded in high resolution (with resolution of a minimum of 100,000 at any wavelength) from the online RG planet spectra catalog upon publication of this study. For ease of comparison in the figures, we rebin the spectra to a resolution of 140 using a triangular smoothing

²<https://www.usgs.gov/labs/spectral-capabilities/spectral-library>

³<https://speclib.jpl.nasa.gov>

kernel. We chose the resolution of 140 for our figures based on instruments on JWST (Gardner et al. 2006) with resolution between 100 and 150 and instrument designs for ARIEL (Tinetti et al. 2016), WFIRST (Green et al. 2012), Origins (Battersby et al. 2018), HabEX (Mennesson et al. 2016), and LUVOIR (Bolcar et al. 2016).

3. Results: spectra of Earth-like planets orbiting red giant hosts

3.1. Spectra of Earth-like planets in the RG HZ receiving modern Earth irradiation

Temperature, chemical mixing ratio profiles (see Figure 2), and UV surface environments for our planet models are described in

detail in Kozakis & Kaltenegger (2019). For all models we keep surface outgassing rates at modern Earth levels for H_2 , CH_4 , CO , N_2O , and CH_3Cl and maintain constant mixing ratios of O_2 at 0.21 and CO_2 at 3.55×10^{-6} (ibid). The surface pressure is set by the initial 1 bar pressure and consequent atmosphere erosion.

We summarize the major model characteristics of that paper here to link them to the atmospheric features that are shown in the spectra and contrast ratios. Planetary surface temperatures increase with decreasing surface temperature of their RGs hosts due to the shift in peak wavelength to longer wavelengths for cool stars and the higher efficiency of surface heating via redder light (see e.g. Kasting et al. 1993). This increase in surface temperature increases the amounts of atmospheric H_2O for our model planets. Planets orbiting hotter RGs receive higher incident UV irradiation, thus show higher ozone (O_3) production, creating more hydroxyl (OH), a by-product of ozone. This leads to lower levels of methane (CH_4) for planets orbiting hotter RGs both due to depletion via OH and higher rates of UV photolysis. Temperature inversion in Earth-like atmospheres is primarily caused by atmospheric heating due to ozone absorption and thus become less pronounced for planets orbiting cooler RGs. CH_4 concentrations increase in our models for cooler RG hosts, where CH_4 heats the upper atmosphere, further reducing temperature inversion. Several studies have found similar results for planets orbiting in the HZ of MS stars with similar stellar surface temperatures (e.g. Segura et al. (2005); Rugheimer et al. (2015)).

Figure 3 shows the planets' reflection and emission spectra. Atmospheric feature depth in reflection spectra is determined by the abundance of the chemical species, while the depth of spectral features in an emis-

sion spectra is set by both the abundance of the chemical as well as the temperature at which a chemical absorbs/emits versus the temperature the overall emitting temperature of the planet. Larger temperature contrast between the emitting/absorbing layer compared to the continuum at that wavelength give more depth to the features for the same chemical abundance. The temperature inversion in the model atmospheres decreases for cooler RG hosts, reducing the depth of the absorption features in emission for cooler RGs. The increasing peak wavelength of the emission for cooler RGs reduces the shortwave incident stellar light and thus the absorption depth of chemicals in reflected light at short wavelength.

Figure 3 shows the spectra of Earth-like planet models orbiting RG hosts at the 1AU equivalent distance, as planetary flux, contrast ratios of the planet to its host star's flux, and the relative absorption of the individual chemicals in the Earth-Sun model for reference, to clarify the overlap of individual spectral lines. These individual chemical plots are generated by removing the opacity of all other molecules from the original atmosphere, and calculating only the opacity due to one particular atmospheric species (see Kaltenegger et al. (2007)).

At a resolution of $R = 140$ all planet spectra show features of H_2O , CO_2 , CH_4 , O_3 and O_2 (Figure 3) H_2O absorption bands are present at 0.9, 1.1, 1.4, 1.9, 5, and 17 μm . The abundance and thus the depth of the visible H_2O absorption features increase with increasing planetary surface temperature for cooler RG hosts. Cooler RG hosts provide lower stellar UV environments, decreasing water photolysis. CO_2 shows absorption features at 2 and 15 μm . The temperature inversion in the model atmospheres decreases for cooler RG hosts, decreasing the inversion indication in the center of the CO_2 absorption

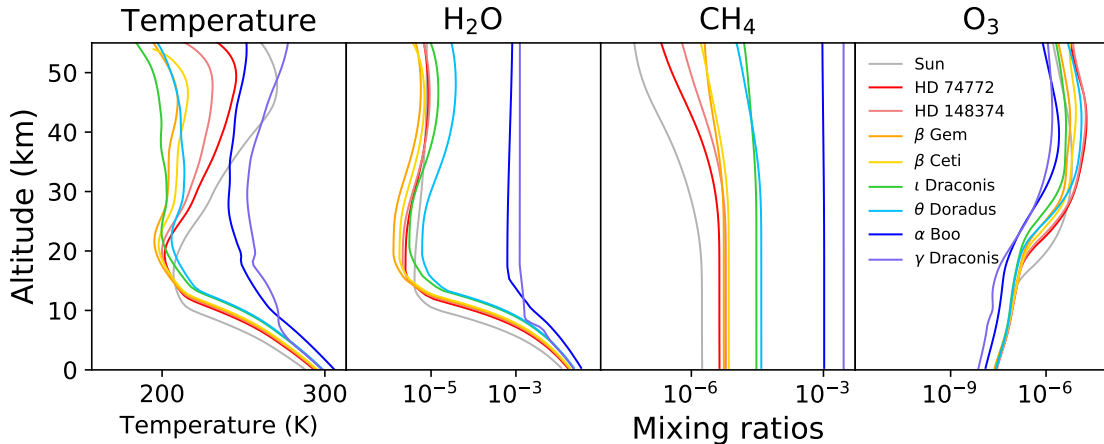


Fig. 2.— Temperature and chemical profiles for Earth-like planet models orbiting red giants with surface temperature between 5200 and 3600 K at the 1 AU equivalent distance (Kozakis & Kaltenegger 2019). RGs are ordered from hottest to coolest in the legend.

feature at $15 \mu\text{m}$ for cooler RG hosts. Hotter RG hosts show increased O_3 production due to higher stellar UV flux, which deepens the $9.6 \mu\text{m}$ O_3 feature because of the larger temperature difference between the hotter stratosphere and the planet’s overall emission temperature for these models. Note that the O_3 feature at $0.6 \mu\text{m}$ in reflected light is very shallow for all models. Absorption features for CH_4 can be seen at 1.7 , 2.4 and $7.7 \mu\text{m}$. CH_4 is depleted both through UV photolysis and reactions with OH (a by-product of O_3), causing shallower feature depth in the reflected light at 1.7 and $2.4 \mu\text{m}$ for hotter RG hosts with more UV. The IR absorption feature at $7.7 \mu\text{m}$ shows more variation due to the additional effect of the decreasing temperature difference between the absorption layer and the overall planet emission temperature for cooler RG host models.

Absorption features for O_2 (or O_3) in combination with CH_4 (see e.g. Lovelock 1965; Lederberg 1965; Lippincott et al. 1967) can indicate life on a planet like Earth. This combination of features can be seen in Figure 3 for all planet models in the RG HZ. The depth

of the O_2 feature at $0.76 \mu\text{m}$ in the reflection spectra becomes difficult to identify at a resolution of 140 for cooler RGs because of the low incident flux level for cool RGs at these wavelengths. As an example of how such features appear in high resolution, Figure 4 shows the absorption features of O_2 at $0.76 \mu\text{m}$ for all planet models at a resolution of $R = 100,000$, which is proposed for several upcoming instruments such HIRES on the ELT (Gilmozzi, & Spyromilio 2007). For ground-based observations Doppler shift due to the motion of the planet compared to terrestrial features can increase the detectability of spectral features in high resolution (e.g. Snellen et al. 2013; Brogi et al. 2014; Birkby 2018).

3.2. Spectra of Earth-like planets in the RG HZ through RG evolution

In this section we discuss the spectra for planet models through their RG’s evolution. Temperature and chemical profiles for all model planets throughout their RGs host star evolution are shown and discussed in (Kozakis & Kaltenegger 2019). We model high

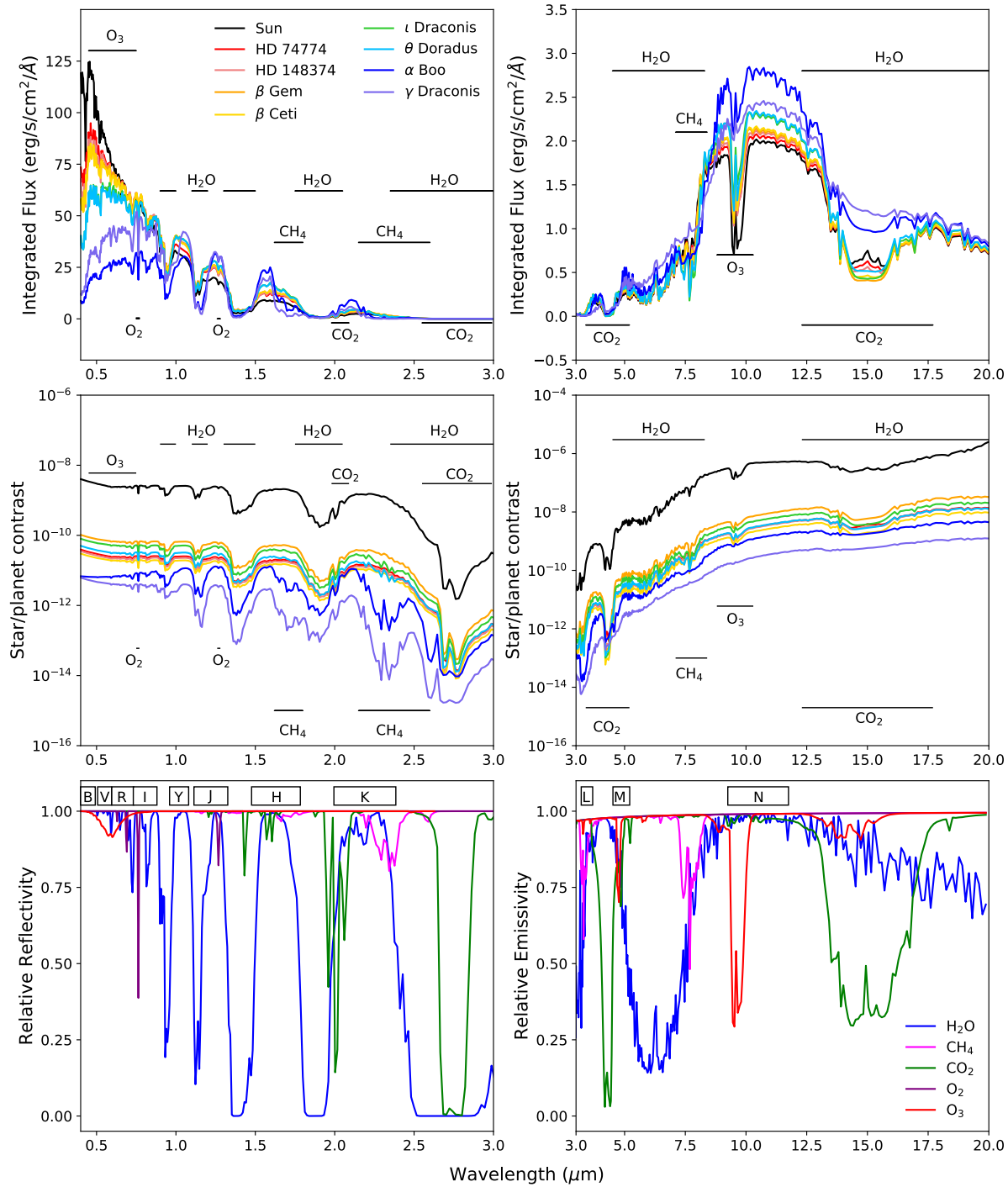


Fig. 3.— Reflection (left) and emission (right) spectra for Earth-like planets orbiting their red giant hosts at the 1 AU equivalent distance. The top row shows the planet’s flux, the middle the contrast ratio between the planet and its host star, and the bottom row the absorption of individual chemical species for the Sun-Earth case for reference. RGs are ordered from hottest to coolest in the legend.

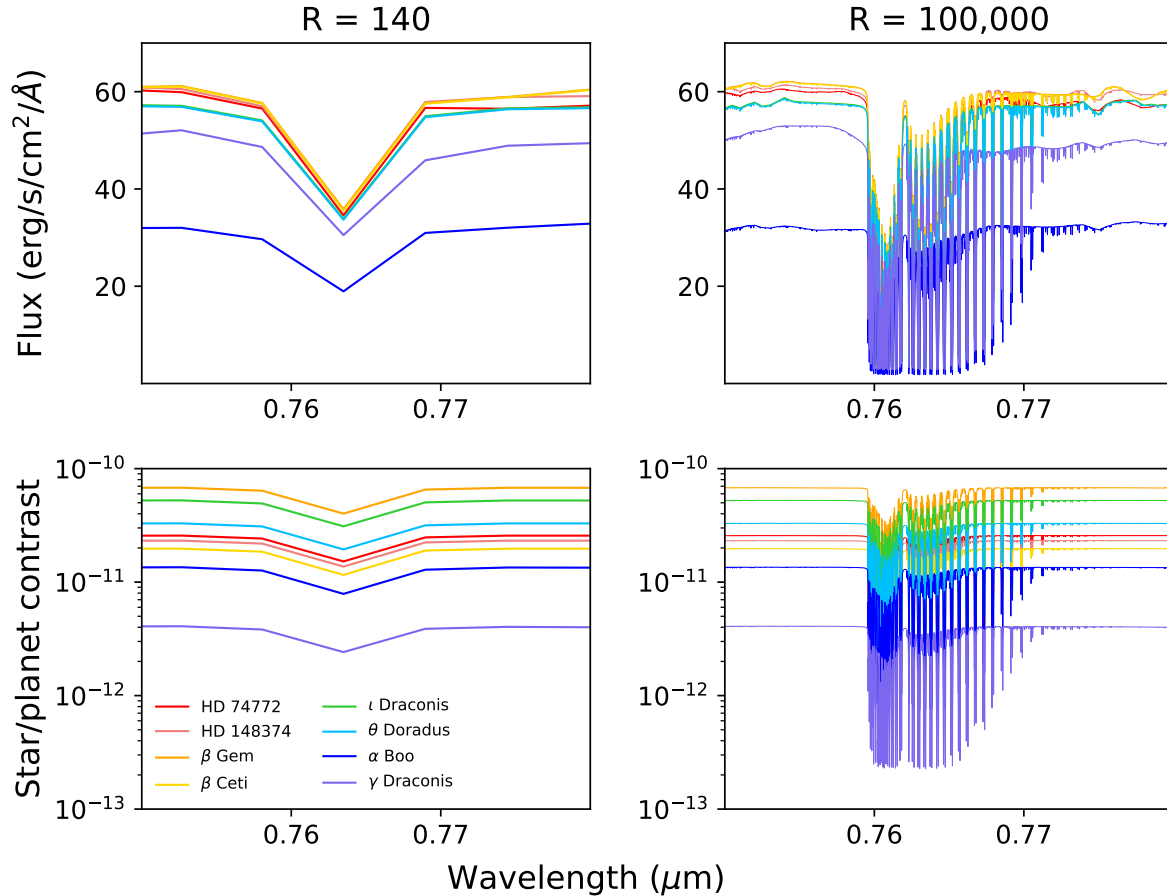


Fig. 4.— O_2 features at $0.76 \mu\text{m}$ as (top) planet flux and (bottom) star/planet contrast shown at a resolution of (left) 140 and (right) at high resolution of 100,000, as proposed for the HIRES instrument on the ELT.

resolution spectra for these planets orbiting RG hosts for 3 mass tracks of 1.3, 2.3, and $3.0 M_{\odot}$ (as discussed in detail in Kozakis & Kaltenegger 2019). For each mass track we model the planetary atmosphere at multiple points on the orbit that provides the planet the maximum amount of time continuously in the RG HZ.

Figure 5 shows the evolution of a model planet’s spectra set at an initial orbital distance of 12.5 AU from a $1.3 M_{\odot}$ host star during its RG evolution in planetary flux and planet-to-star contrast ratio as an example for the 3 RG mass tracks modeled. The points in time modeled are shown as star markers

on the RG’s evolutionary track in the top row. The red zone indicates the RG phase, the blue zone the AGB, and the green zone the time that the specific model planet spends in the HZ during the RG’s evolution. Planet spectra for all 3 mass tracks can be downloaded in high resolution from our online spectral database which will become available when this study is published.

These planets spend the majority of their time in the RG HZ orbiting near the outer edge of the RG HZ where the overall incident irradiation is low (Figure 5 top right). As a result these planet models initially have cold surface temperatures because we did not

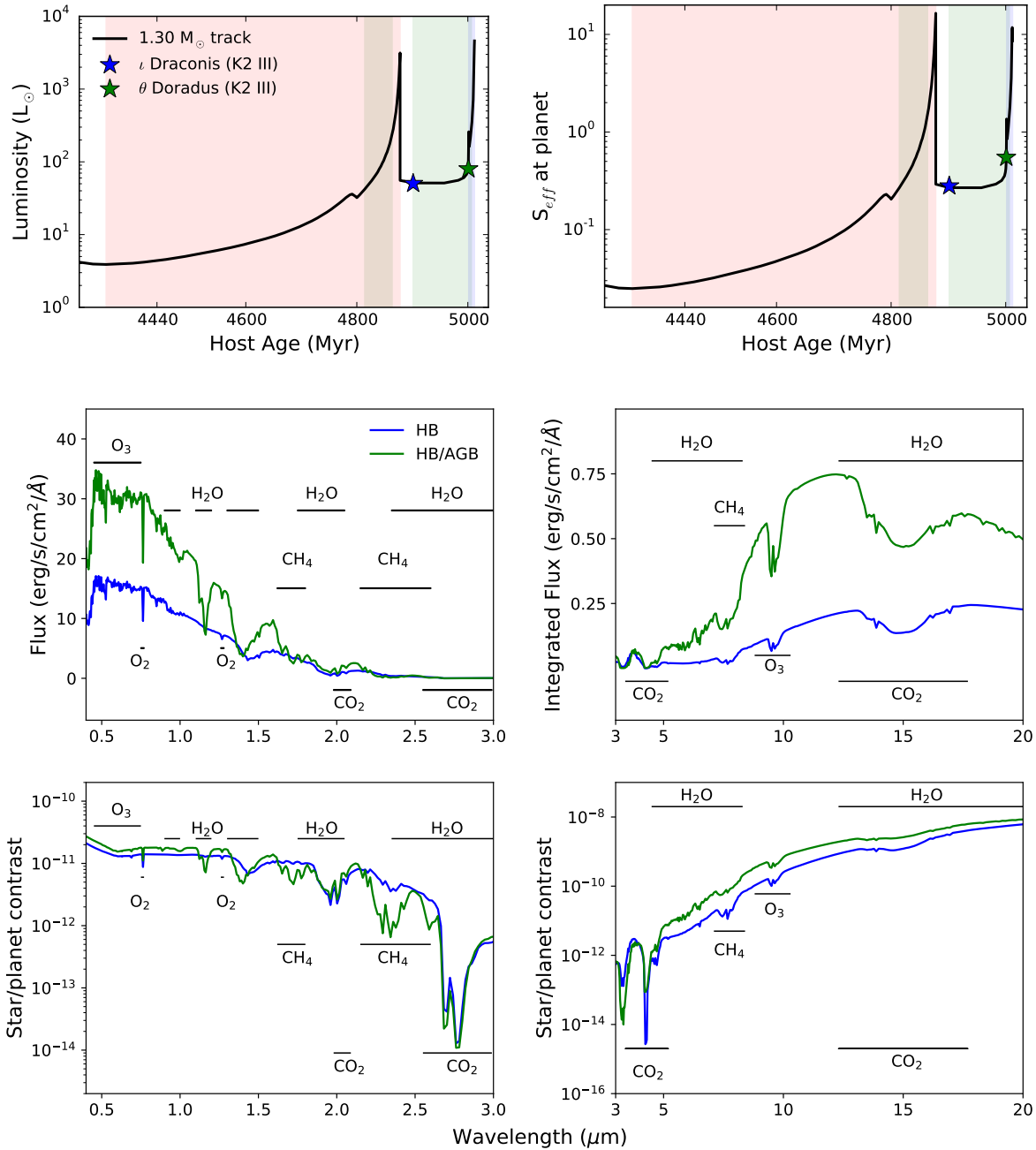


Fig. 5.— Luminosity evolution and spectra of a planet in the HZ of a $1.3 M_{\odot}$ red giant on the orbit giving the maximum amount of time in the RG HZ. The top row shows (left) the luminosity evolution of the red giant host and (right) the changing incident flux upon the planet on an orbit giving it maximum time in the habitable zone. The quantity S_{eff} is the fraction of flux received by the planet compared to modern Earth. The modeled points of evolution are marked with stars. The middle and bottom rows show the spectra of this planet throughout evolution and the star/planet contrast ratios.

change the CO_2 concentration in these mod-

els for ease of comparison. Assuming rocky

planets in the HZ of RGs could maintain a carbonate silicate cycle until the RG phase of their host, these planets should maintain higher CO₂ concentration in their atmosphere (see e.g. review Kaltenegger 2017). However no there are no models which explore whether the carbonate-silicate or similar cycles could be maintained on frozen planets until the RG phase of their host. Therefore we maintained a modern Earth-analog concentration of CO₂ in our planet models, which initially produce cold environments until the RGs luminosity increases sufficiently to warm the planet.

Cold planetary atmospheres generally have lower H₂O abundance, resulting in initially shallower H₂O spectral features, which become more pronounced with a RGs increasing luminosity and the resulting increase in planetary surface temperature. In the reflected spectra the increase is due to the increasing H₂O abundance, while in the emission spectra the increasing H₂O abundance as well as the increasing planet emission temperature deepen the absorption features.

Increasing UV incident flux on the planets over the RG’s evolution increases the O₃ abundance and decreases the CH₄ abundance in the planets’ atmospheres. These model planets initially have low amounts of reflected flux due to the smaller incident amounts of RG host flux they reflect and lower emitted flux due to the low planetary surface temperatures. With increasing incident irradiation at the planet’s orbital position from the RG through its evolution (Figure 5 top right), the planet’s reflected flux increases. The planet’s emitted flux also increases due to the increasing surface temperature. Thus a planet in the HZ of a RG displays increasing depth of spectral features in both emitted and reflected flux with its RG’s evolution.

4. Discussion and Conclusions

While attention is focused on planets orbiting in the HZ of MS stars, detected exoplanets orbiting RG hosts raise the question of the nature of life and how to characterize it on such planets. Here we present high resolution reflection and emission spectra from 0.4 to 20 μm for models of Earth-like planets orbiting in the HZ of RGs shown in Figures 3 and 5. All model spectra show atmosphere features of H₂O, CO₂, CH₄, O₃ and O₂ at a resolution of 140. All spectra are calculated at minimum resolution of 100,000 at all wavelengths. Figure 4 shows the absorption feature of O₂ at 0.76 μm in reflected light at a resolution of 100,000 as proposed for spectrographs like HIRES at ELTs.

The orbital distance of the RG HZ increases significantly due to the higher luminosity of the host RG, increasing the apparent angular separation of such planets compared to MS HZ planets. Yet the contrast ratio between such planets and their RG hosts are smaller than for similar planets orbiting in the HZ of MS stars because of the RG’s increased luminosity. However ground-based high resolution spectroscopy has already characterized atmospheric species for unresolved planets like HD 179949 b using the planet’s known motion during the observations. A similar approach could be used to counter the increased luminosity of RG hosts to observe their HZ planets, making such planets interesting targets for the Extremely large Telescopes like the ELT, GMT and TMT.

We present our spectra noise-free to serve as input for simulations of observations for ground- and space-based telescopes. Observation time for specific features will depend in addition on the stellar noise and the properties and systematics of the observing instrument. All spectra are available in

high resolution online upon publication of this study and can be put through a variety of noise simulators to plan observations.

This work was supported by the Carl Sagan Institute. T.K. was additionally funded by a NASA Space Grant fellowship.

REFERENCES

- Battersby, C., Armus, L., Bergin, E., et al. 2018, *Nature Astronomy*, 2, 596
- Barnes, R., & Heller, R. 2013, *Astrobiology*, 13, 279
- Birkby, J. L. 2018, *Handbook of Exoplanets*, 16
- Bolcar, M. R., Feinberg, L., France, K., et al. 2016, *Proc. SPIE*, 9904, 99040J
- Brogi, M., de Kok, R. J., Birkby, J. L., et al. 2014, *A&A*, 565, A124
- Danchi, W. C., & Lopez, B. 2013, *ApJ*, 769, 27
- Des Marais, D. J., Harwit, M. O., Jucks, K. W., et al. 2002, *Astrobiology*, 2, 153
- Furnes, H., Banerjee, N. R., Muehlenbachs, K., et al. 2004, *Science*, 304, 578
- Gardner, J. P., Mather, J. C., Clampin, M., et al. 2006, *Space Sci. Rev.*, 123, 485
- Gilmozzi, R., & Spyromilio, J. 2007, *The Messenger*, 127, 11
- Green, J., Schechter, P., Baltay, C., et al. 2012, *arXiv e-prints*, arXiv:1208.4012
- Grunblatt, S., Huber, D., Lopez, E., et al. 2017, *Spitzer Proposal*, 13237
- Jiang, J. H., & Zhu, S. 2018, *Research Notes of the American Astronomical Society*, 2, 185
- Jones, M. I., Jenkins, J. S., Bluhm, P., et al. 2014, *A&A*, 566, A113
- Kaltenegger, L. 2017, *ARA&A*, 55, 433
- Kaltenegger, L., Sasselov, D., & Rugheimer, S. 2013, *ApJ*, 775, L47
- Kaltenegger, L., Selsis, F., Fridlund, M., et al. 2010, *Astrobiology*, 10, 89
- Kaltenegger, L., Traub, W. A., & Jucks, K. W. 2007, *ApJ*, 658, 598
- Kasting, J. F., Whitmire, D. P., & Reynolds, R. T. 1993, *Icarus*, 101, 108
- Kozakis, T., & Kaltenegger, L. 2019, *ApJ*, 875, 99
- Kozakis, T., Kaltenegger, L., & Hoard, D. W. 2018, *ApJ*, 862, 69
- Lederberg, J. 1965, *Nature*, 207, 9
- Lippincott, E. R., Eck, R. V., Dayhoff, M. O., et al. 1967, *ApJ*, 147, 753
- Lopez, E. D., & Fortney, J. J. 2016, *ApJ*, 818, 4
- Lopez, B., Schneider, J., & Danchi, W. C. 2005, *ApJ*, 627, 974
- Lorenz, R. D., Lunine, J. I., & McKay, C. P. 1997, *Geophys. Res. Lett.*, 24, 2905
- Lovelock, J. E. 1965, *Nature*, 207, 568
- Mennesson, B., Gaudi, S., Seager, S., et al. 2016, *Proc. SPIE*, 9904, 99040L
- Pickles, A. J. 1998, *PASP*, 110, 863
- Ramirez, R. M., & Kaltenegger, L. 2016, *ApJ*, 823, 6
- Rugheimer, S., Kaltenegger, L., Segura, A., et al. 2015, *ApJ*, 809, 57

- Segura, A., Kasting, J. F., Meadows, V., et al. 2005, *Astrobiology*, 5, 706
- Snellen, I. A. G., de Kok, R. J., le Poole, R., Brogi, M., & Birkby, J. 2013, *ApJ*, 764, 182
- Schwieterman, E. W., Kiang, N. Y., Parenteau, M. N., et al. 2018, *Astrobiology*, 18, 663
- Stern, S. A. 2003, *Astrobiology*, 3, 317
- Stock, S., Reffert, S., & Quirrenbach, A. 2018, *A&A*, 616, A33
- Tinetti, G., Drossart, P., Eccleston, P., et al. 2016, *Proc. SPIE*, 99041X
- Traub, W. A., & Stier, M. T. 1976, *Appl. Opt.*, 15, 364
- Yang, J., Ding, F., Ramirez, R. M., et al. 2017, *Nature Geoscience*, 10, 556